THE JOURNAL OF BIOLOGICAL CHEMISTRY VOL. 286, NO. 8, pp. 6329–6335, February 25, 2011

Rotational Position of a 5-Methylcytosine-containing Cyclobutane Pyrimidine Dimer in a Nucleosome Greatly Affects Its Deamination Rate*[S]

Received for publication, September 8, 2010, and in revised form, December 9, 2010 Published, JBC Papers in Press, December 15, 2010, DOI 10.1074/jbc.M110.183178

Qian Song, Vincent J. Cannistraro, and John-Stephen Taylor[1]

From the Department of Chemistry, Washington University, St. Louis, Missouri 63130

C to T mutation hotspots in skin cancers occur primarily at methylated CpG sites that coincide with sites of UV-induced cyclobutane pyrimidine dimer (CPD) formation. These mutations are proposed to arise from the insertion of A by DNA polymerase η opposite the T that results from deamination of the methylC (^{m}C) within the CPD. Although the frequency of CPD formation and repair is modestly modulated by its rotational position within a nucleosome, the effect of position on the rate of ^{m}C deamination in a CPD has not been previously studied. We now report that deamination of a T^{m}C CPD whose sugar phosphate backbone is positioned against the histone core surface decreases by a factor of 4.7, whereas that of a T^{m}C CPD positioned away from the surface increases by a factor of 8.9 when compared with unbound DNA. Because the ^{m}Cs undergoing deamination are in similar steric environments, the difference in rate appears to be a consequence of a difference in the flexibility and compression of the two sites due to DNA bending. Considering that formation of the CPD positioned away from the surface is also enhanced by a factor of two, a T^{m}CG site in this position might be expected to have up to an 84-fold higher probability of resulting in a UV-induced ^{m}C to T mutation than one positioned against the surface. These results indicate that rotational position may play an important role in the formation of UV-induced C to T mutation hotspots, as well as in the mutagenic mechanism of other DNA lesions.

Sunlight is a major epidemiological factor for the induction of skin cancer. In basal and squamous cell carcinomas, the p53 tumor suppressor gene exhibits a very high percentage of C to T transition mutations at dipyrimidine sites, including the tandem CC to TT mutation (1–4). The UVB wavelengths in sunlight induce the formation of many types of photoproducts at dipyrimidine sites in DNA, the majority of which are cyclobutane pyrimidine dimers (CPDs)[2] (5–8). Methylation of C at 5′-PyCG sites further enhances formation of CPDs 15-fold in sunlight (9, 10), and most C to T mutation hotspots occur at methylated 5′-PyCG sites (10–12). It has been found that 5-methylcytosine is involved in 25–40% of sunlight-induced mutations of the *cII* and *lacI* transgenes as well as the p53 gene in skin tumors and that CPDs are responsible for a significant fraction of these mutations (6, 13).

The initially formed cyclobutane pyrimidine dimers are not significantly mutagenic, however, because of the DNA damage bypass polymerase η, which can efficiently bypass T- and C/^{m}C-containing dimers in an essentially error-free manner (14–17). Although the T in a CPD is stable, the C and ^{m}C are not, and they deaminate to U and T in a matter of hours or days (18–24) (Fig. 1), unlike their canonical forms, which deaminate with a half-life of about 50,000 years (25, 26). Deamination of Cs or ^{m}Cs in CPDs is highly mutagenic because polymerase η will faithfully insert A opposite the resulting Us or Ts, thereby producing the observed C to T and CC to TT mutations (the deamination-bypass mechanism) (3, 4, 27–29). The frequency of C to T and CC to TT mutations will depend, however, on the rate of formation of C-containing dimers, their rate of repair, deamination, and bypass by polymerases. All of these processes are expected to be modulated by sequence context, protein interactions, as well as the secondary and tertiary structure of DNA. A detailed understanding of all these processes and interactions may lead to a better understanding of the origin of UV mutation hotspots.

Nucleosomes are the primary structural unit of chromatin in eukaryotic cells (30). Nucleosome core particles contain about 150 bp of DNA, which wrap 1.7 times around a histone octamer, made up of two H2A, H2B, H3, and H4 histones (31). UV preferentially induces the formation of CPDs in nucleosomes at sites where the phosphodiester backbone is positioned away from the histone surface and DNA bending is toward the major groove (32, 33). This preference is also seen for bent DNA that is not in contact with a protein (34) and has been attributed to the greater degree of rotational freedom in the phosphate backbone, making it easier to for adjacent pyrimidines to adopt a photoreactive conformation (35, 36). When DNA containing randomly distributed CPDs is assembled into nucleosomes, the CPDs also favor positions away from the surface (37), which is consistent with the 30° bend that they make toward the major grove of DNA (38). Despite the distortion of DNA caused by CPDs, nucleosome core particles containing CPDs in different rotational settings can be readily prepared and isolated (39–41).

Nucleosomes have also been found to affect the repair of CPDs (42). *In vitro* studies with human fibroblast extracts

* This work was supported, in whole or in part, by National Institutes of Health Grant CA40463 (to J.-S. T.).

[S] The on-line version of this article (available at http://www.jbc.org) contains supplemental Figs. S1–S6.

[1] To whom correspondence should be addressed. Tel.: 314-935-6721; Fax: 314-935-4481; E-mail: taylor@wustl.edu.

[2] The abbreviations used are: CPD, cyclobutane pyrimidine dimer; ^{m}C, methylC; dC, deoxycytidine; ODN, oligodeoxynucleotide; NCP, nucleosome core particle; TBE, Tris-borate-EDTA.

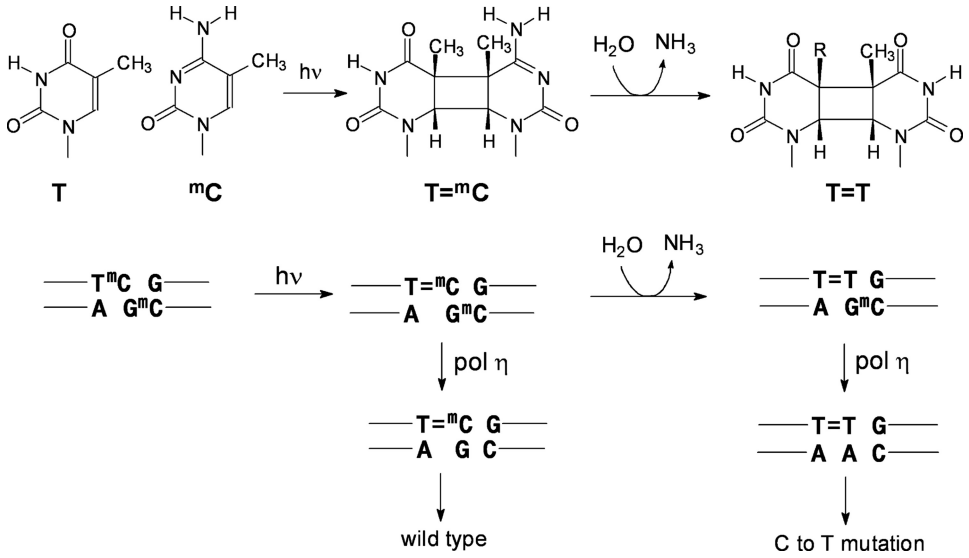

FIGURE 1. **Mutagenic properties of ^{m}C-containing *cis-syn*-cyclobutane dimers and their deamination products.** *Upper*, UVB irradiation of a T^{m}C site leading to a *cis-syn*-T=^{m}C CPD followed by deamination to give the *cis-syn*-cyclobutane dimer of T=T. *Lower*, mutagenic consequences of bypass of a T=^{m}C CPD and its deamination product, T=T by polymerase η (*pol η*).

found that nucleosomes reduce the rate of nucleotide excision repair of CPDs by 6–9-fold relative to free DNA (43). A similar 10-fold reduction in excision repair has been observed for a site-specific CPD reconstituted with human nucleosome core particles (44). With *Xenopus* nuclear extracts, the nucleotide excision repair rates of rotationally positioned CPDs were only 2–3 times lower in nucleosomes and no more than 1.5-fold greater when a CPD was positioned away from the histone surface when compared with against the surface (41). In an earlier study with a 5S rRNA gene, no correlation was observed with rotational positioning of the CPD (45).

Although the effects of nucleosome positioning on the rates of CPD formation and repair have been studied, the effects on the deamination rates of C- and ^{m}C-containing CPDs have not. The purpose of this study was to determine the extent to which the rotational position of the CPD relative to the histone surface affects the rate of ^{m}C to T deamination, and hence, its potential mutagenicity by a deamination bypass mechanism. To address this question, we determined the deamination rate of a T^{m}CG CPD in two different orientations in a nucleosome core particle. We find that a T^{m}C CPD positioned against the surface deaminates 4.7 times slower than the unbound sequence, whereas a T^{m}C CPD facing out deaminates 8.9 times faster than the unbound sequence, corresponding to an overall 42-fold difference in rate.

EXPERIMENTAL PROCEDURES

DNA Substrates—Oligodeoxynucleotides with or without 5′-terminal phosphates were purchased from Integrated DNA Technologies and purified by denaturing gel electrophoresis prior to ligation with T4 DNA ligase and ATP in the presence of complementary 20-mer ligation scaffolds (supplemental Figs. S1 and S2). The 150-mer single strand products were purified by denaturing PAGE. Complementary 150-mers were then annealed to form the 150-mer duplexes and purified by native PAGE (supplemental Fig. S3).

Nucleosome Reconstitution—Nucleosome core particles were isolated and purified from chicken erythrocytes following a detailed procedure provided by the Dr. Michael Smerdon laboratory. Each 150-mer DNA duplex (ds-IN, ds-OUT, and ds-control) was reconstituted with the chicken nucleosome core particles by slow dialysis from high to low salt as described previously (46). Briefly, about 10 nM 150-mer duplex was incubated with an increasing amount of nucleosome core particles (from 100 to 500 nM) in a total volume of 500 μl, containing 2 M NaCl, 10 mM Tris-HCl, 5 mM EDTA at pH 7.5 and room temperature for 2 h, and then dialyzed against 50 mM NaCl, 10 mM Tris-HCl, pH 7.5, at 4 °C, overnight. Finally, the reconstituted particles were recovered from the dialysis tubing and equilibrated at 55 °C for 2 h to fix the nucleosome phasing. The reconstituted particles were assayed by native PAGE (6% acrylamide, 0.2% bisacrylamide in TBE), and the ratio of nucleosome-bound DNA to free DNA was quantified by the Quantity One software (supplemental Fig. S4).

Hydroxyl Radical Footprinting and Dimethylsulfate Mapping—Hydroxyl radical footprinting was performed as described previously (46). Briefly, a 15-μl aliquot of 10 mM sodium ascorbate, a 15-μl aliquot containing 1 mM $Fe(NH_4)_2(SO_4)_2{\cdot}6H_2O$ and 2 mM EDTA, and 15 μl of a 0.12% (w/w) H_2O_2 solution were premixed and added within 5 s to 105 μl of the nucleosome-bound DNA sample. The reaction was incubated for 120 s at room temperature and stopped by the addition of 16 μl of 50% (v/v) glycerol and 4 μl of a 500 mM EDTA solution. The samples were electrophoresed on a native gel (6% acrylamide, 0.2% bisacrylamide in TBE), and the nucleosome bands were electroeluted in TBE. The proteins were extracted with phenol:chloroform:isopropyl alcohol 25:24:1, and the DNA was precipitated with ethanol. The free ds-control was treated in a similar way, except that the reaction was quenched with a solution containing 1 M sodium acetate, 120 mM thiourea, 300 μg/ml salmon sperm DNA, and

60 mM EDTA at pH 6.5 and then ethanol-precipitated. A Maxam-Gilbert G sequencing reaction was also carried out on the free ds-control in 50 mM cacodylate, 50 mM NaCl, 5 mM EDTA in the presence of 10 nM ds-control. For a 50-μl reaction, 0.5 μl of dimethyl sulfate was added to initiate the reaction, and 10-μl aliquots were removed over time and quenched by the addition of 50 μl of 1.5 M sodium acetate, 1 M mercaptoethanol and 50 μg of denatured salmon sperm DNA. The samples were ethanol-precipitated twice, and the resulting pellets were vacuum-dried and then solubilized in 100 μl of 1 M piperidine. The samples were then heated at 90 °C in 1 M piperidine for 30 min and then evaporated to dryness at 60 °C.

Deamination Rate Assay by Two-dimensional Gel Electrophoresis—The deamination rate was determined by adapting a previously described method (24). The free and nucleosome-bound internally ^{32}P-labeled 150-mer ds-IN and ds-OUT were irradiated with 302 nm UVB light at 4 °C for 1 h and then adjusted to pH 7.2 with Mes buffer (0.5 M) and incubated at 37 °C. Aliquots (10-μl) were removed at various times and quickly frozen on dry ice before storing overnight at −70 °C. The remaining sample was adjusted to pH 6.5 with Mes buffer (0.5 M) and heated at 67 °C overnight to complete the deamination. The aliquots were then warmed to room temperature, extracted with phenol:chloroform:isopropyl alcohol 25:24:1, ethanol-precipitated, redissolved in buffer, and photoreverted with photolyase and 365 nm light for 1 h. After photoreversion, the aliquots were treated with nuclease P1 to degrade the DNA to mononucleotides containing either ^{32}P-^{m}dC or ^{32}P-T, depending on the extent of deamination, and separated by two-dimensional gel electrophoresis. In the first dimension, electrophoresis on a 7 M urea, a TBE gel was used to separate ^{32}P-^{m}dC and ^{32}P-T, which co-migrate, from partially digested material and protein. For the second dimension, the gel surrounding the radioactive band containing the mononucleotides was excised, and a second gel containing 25 mM citric acid, pH 3.5, and 7 M urea was poured around the remaining gel slice. Electrophoresis on this gel separated ^{32}P-^{m}dC from ^{32}P-T with the ^{32}P-T migrating the fastest. The deamination rate constant was obtained from the slope of a linear least squares fit of the log of the fraction of remaining T^{m}C CPD *versus* deamination time (supplemental Figs. S5 and S6). The fraction of T^{m}C CPD remaining was calculated as $1 - (T/(T + {}^{m}C))/(T_\infty/(T_\infty + {}^{m}C))$ where $T_\infty/(T_\infty + {}^{m}C_\infty)$ is the fraction $T/(T + {}^{m}C)$ in the fully deaminated sample. The yield of CPD photoproduct was calculated as the $T_\infty/(T_\infty + {}^{m}C_\infty) - T_0/(T_0 + {}^{m}C_0)$, where $T_0/(T_0 + {}^{m}C_0)$ is the fraction $T/(T + {}^{m}C)$ at time 0.

RESULTS

Design and Synthesis of the DNA Substrates—The substrate for study was adapted from a previously described 150-mer sequence that was shown by hydroxyl radical footprinting to position a TT CPD near the dyad axis with an inside (IN) or outside (OUT) orientation relative to the histone core surface (41). The CPDs were oriented by flanking the dimer-containing sequence with multiple TG motifs $(T/A)_3NN(G/C)_3$ that had been shown to position a glucocorticoid hormone-response element (GRE) with different orientations relative to the histone surface (47, 48). To study the effect of the CPD position on the deamination of cyclobutane pyrimidine dimers of T^{m}CG sites, we simply replaced the ATTA (OUT) and GTTC (IN) CPD sites in the original 150-mer sequence with AT^{m}CG and GT^{m}CG sites respectively (see Fig. 3, *top right*).[3]

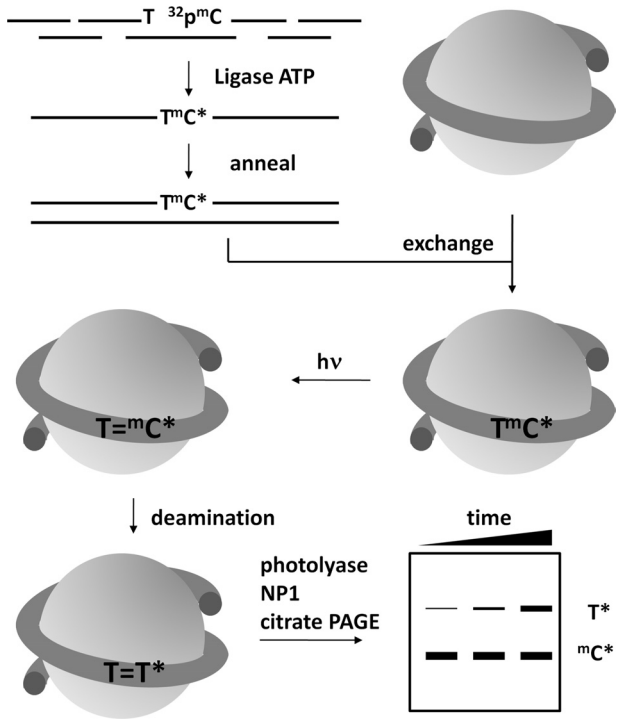

FIGURE 2. **Strategy for determining the deamination rates of T^{m}CG CPDs in a nucleosome core particle.** A 150-mer DNA duplex was constructed by first assembling each strand from four ODNs by ligation in the presence of three complementary 20-mer ligation scaffolds where the ODN containing the ^{m}C site of interest was 5′-end-labeled with [γ-^{32}P]ATP and kinase prior to ligation. The internally labeled 150-mer duplex was assembled into isolated nucleosome core particles through an exchange reaction, irradiated with UVB light, and allowed to deaminate. At specific times, the protein was removed by phenol extraction, and the *cis-syn*-CPDs were photoreverted with photolyase, degraded with nuclease P1, subjected to two-dimensional gel electrophoresis to separate the radiolabeled T from undeaminated radiolabeled ^{m}dC, and quantified by radioisotopic imaging analysis.

To determine the deamination rates of the T^{m}C CPDs, we used a previously developed method that requires the ^{m}C to be 5′-^{32}P-end-labeled (Fig. 2) (24). We therefore prepared the two internally ^{32}P-labeled duplex 150-mers, ds-IN and ds-OUT, along with a 5′-end-labeled control duplex, ds-control. The duplexes were prepared by annealing complementary single strand 150-mers that were prepared by ligating four ODNs together with T4 ligase and ATP in the presence of complementary ligation scaffolds (Fig. 2). For ds-IN and ds-OUT, the second and third ODNs of the top strand were designed so that the ^{m}C of interest would be at the 5′-end of the third fragment so that the ^{m}C could be 5′-^{32}P-end-labeled prior to ligation (supplemental Figs. S1 and S2). Thus, ds-IN was ^{32}P-labeled at the ^{m}C of the GT^{m}CG site, ds-OUT was

[3] The IN and OUT substrates were mislabeled in the materials and methods section of the original publication (41), as described in a recent erratum statement.

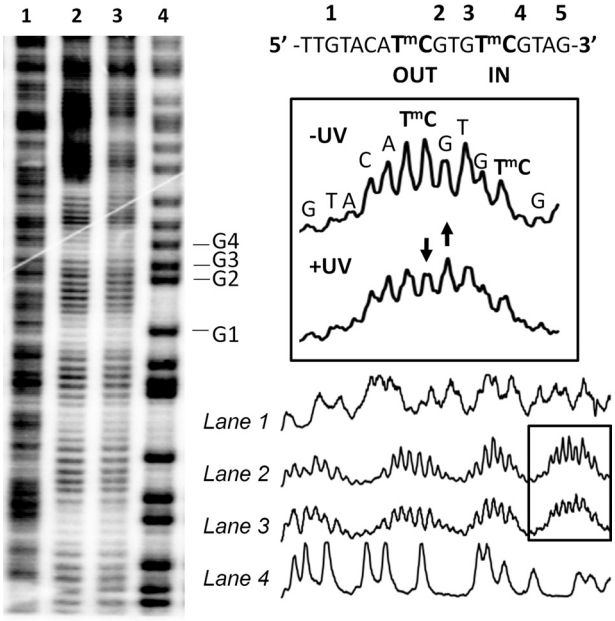

Lane 1: ds-control *Lane 2:* NCP + ds-control
Lane 3: NCP + ds-control + UV *Lane 4:* DMS + ds-control

FIGURE 3. **Hydroxyl radical footprinting of the reconstituted nucleosome core particles to determine phasing.** The nucleosome core particle reconstituted with 5′-end-labeled 150-mer duplex DNA was subjected to hydroxyl radical footprinting and electrophoresed on a 7 M urea, 10% acrylamide, 0.3% bisacrylamide denaturing gel. *Lane 1*, footprinting of the free DNA duplex; *lane 2*, footprinting of the nucleosome-bound DNA duplex; *lane 3*, footprinting of the nucleosome-bound duplex DNA after 1 h of irradiation at 302 nm at 4 °C; *lane 4*, Maxam Gilbert G reaction on the free duplex. *DMS*, dimethyl sulfate.

labeled at the ^{m}C of the AT^{m}CG site, and ds-control was labeled at the 5′-end of the 150-mer of the top strand. Each single strand 150-mer was purified by denaturing PAGE, and the final 150-mer duplexes were purified by native PAGE (supplemental Fig. S3).

Nucleosome Core Particle Reconstitution with the 150-mer DNA Duplexes—The 150-mer duplexes, ds-IN, ds-OUT, and ds-control, were assembled into nucleosome core particles according to a previously described procedure that involves exchanging the DNA with that from chicken erythrocyte nucleosome core particles (NCPs) (39). The 150-mer duplexes were titrated with the NCPs and electrophoresed on a native gel to determine the NCP concentration needed to achieve maximal incorporation of the DNA into the NCP (supplemental Fig. S4). We found that about 90% of 10 nM 150-mer could be incorporated into 500 nM nucleosome core particles.

Orientation of the Two T^{m}C Sites on the Nucleosome Core Particle—To verify the IN and OUT positions of the GT^{m}CG and AT^{m}CG sites, the nucleosomes were analyzed by hydroxyl radical footprinting. The hydroxyl radical cleavage intensity on the nucleosome-bound ds-control with and without UVB irradiation exhibited very pronounced 10–11-bp periodicity with the same phasing as described previously for the ATTA and GTTC sites within the same 150-mer sequence (41) (Fig. 3, *lanes 2* and *3*) when compared with the free ds-control (Fig. 3, *lane 1*). The cleavage sites were mapped onto the sequence by alignment with the Maxam Gilbert G sequencing reaction bands (Fig. 3, *lane 4*). Hydroxyl radicals primarily attack the H5′5″ and H4′ hydrogens that are present on the minor groove side of the DNA (49). The ^{m}C of the AT^{m}CG CPD site is in the center of a region of maximal cleavage, indicating that its phosphodiester backbone is facing out (Fig. 3, *boxed section*). The ^{m}C of the GT-^{m}CG CPD site, which is half a turn from the first site, is at a site of minimal cleavage, indicating that its backbone is facing toward the histone surface.

The similar hydroxyl radical cleavage pattern in the presence and absence of UVB irradiation suggests that the UVB photoproducts do not disrupt the phasing. Furthermore, the decrease of the intensity of the ^{m}C band and increase in that of the flanking G at the AT^{m}CG site following UVB radiation is consistent with the formation of a significant amount of CPD photoproduct (Fig. 3, *boxed section*). It has been previously observed that hydroxyl radical cleavage is suppressed at the 3′-T of a TT CPD and increased at the nucleotide immediately following the 3′-T (41).

Deamination Rates of the Two T^{m}C CPDs—The deamination rates for the IN and OUT T^{m}C CPDs when compared with free DNA were determined by following the conversion of ^{32}P-^{m}dC to ^{32}P-T in the dimer by an enzyme-coupled two-dimensional gel electrophoresis assay (24). In the first step, free or NCP complexed ds-IN and ds-OUT were irradiated with 302 nm light to produce the *cis-syn*-cyclobutane pyrimidine dimers of the AT^{m}CG and GT^{m}CG sites, along with other photoproducts, at 4 °C to suppress deamination. The samples were then incubated at 37 °C and pH 7.2 to allow for deamination for various times, and one was made to undergo complete deamination by lowering the pH and heating. The aliquots were then incubated with *Escherichia coli* photolyase and visible light to specifically photorevert the *cis-syn*-CPDs and then treated with nuclease P1 to degrade all of the undamaged and photoreverted DNA to mononucleotides. Non-photorevertible dipyrimidine photoproducts, such as (6-4) and Dewar photoproducts, would only be digested to trinucleotides. The mononucleotides were then isolated by electrophoresis on a denaturing gel and subjected to a second electrophoresis on a pH 3.5 citrate gel (Fig. 4, *A* and *B*) that separates the ^{32}P-T from the ^{32}P-^{m}dC and quantified by radioisotopic imaging analysis.

The rate constants for deamination were then determined from the slopes of lines fit to the log of the fraction of remaining T^{m}C CPD (supplemental Figs. S5 and S6) as described under "Experimental Procedures" for multiple experiments and then averaged. The photoproduct yields were determined from the increase in the initial amount of radiolabeled T following complete deamination. The initial amount of T was non-zero in many cases and could be attributed to unintended labeling of the T at the 5′-end of the 150-mer resulting from incomplete heat deactivation of the kinase used to label the ^{m}C-containing ODN prior to ligation. Table 1 shows the deamination half-lives and yields of the CPDs in the IN and OUT positions of free and nucleosome-bound DNA. When compared with the free DNA, the nucleosome decreases the rate of deamination of the IN CPD by a factor of 4.7, whereas it increases the rate of deamination of the OUT CPD by a factor of 8.9. We also determined that although

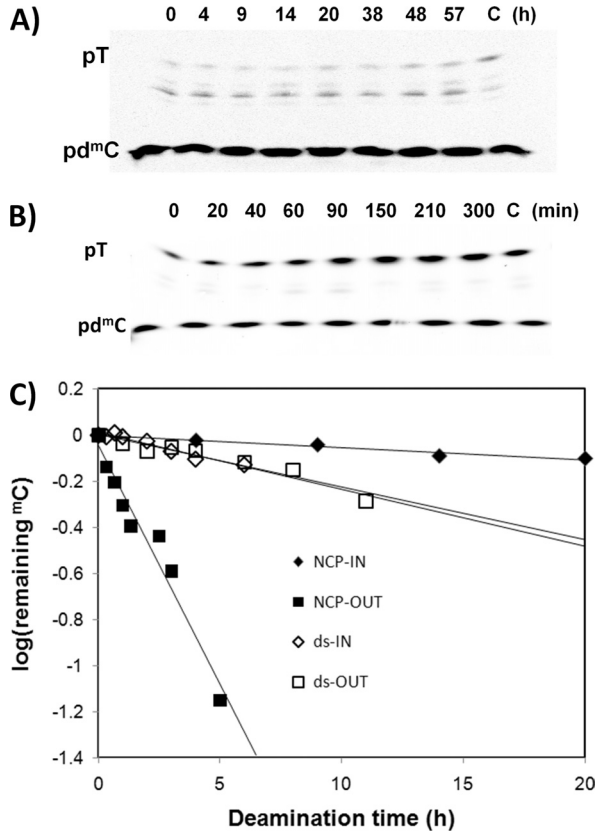

FIGURE 4. **Deamination of the T=^{m}C CPDs in the free and nucleosome-bound 150-mer DNA duplexes.** Free or nucleosome-reconstituted 150-mer DNAs with internal 5′-^{32}P-^{m}dC labeling were irradiated for 1 h with 302 nm light and then allowed to deaminate for the indicated times in hours, after which they were phenol-extracted, photoreverted with *E. coli* photolyase, and then degraded with nuclease P1. The degradation products were first run on a 7 M urea, 10% acrylamide, 0.3% bisacrylamide gel in TBE (first dimension, downward direction) after which the band containing primarily mononucleotides was run on a 25% acrylamide, 0.8% bisacrylamide gel in 25 mM citric acid, pH 3.5 (second dimension, upward direction). *A*, representative second dimension gel of nucleosome-bound 150-mer ds-IN. *B*, representative second dimension gel of nucleosome-bound 150-mer ds-OUT. *C*, plots of log (fraction of T^{m}C CPD remaining) as a function of different deamination times for the gels shown in *A* and *B* and for the free 150-mer ds substrates, after correcting for background ^{32}P-T. Plots for other sets of independent measurements are given in supplemental Figs. S5 and S6. The intermediate bands in the gels shown in *A* and *B* are due to non-photorevertible photoproduct-containing trinucleotides and incomplete digestion products and do not significantly affect the rate measurements.

TABLE 1

Yields and deamination half lives of the T^{m}C CPDs in free and nucleosome-bound DNA (37 °C, 50 m NaCl)

	Photoproduct yield[a]		Deamination half-lives[b]	
	ds-IN (%)	ds-OUT (%)	ds-IN $t_{½}$	ds-OUT $t_{½}$
	%		*h*	
Free	5.5, 5.5	13, 12	12.2 ± 0.9 h	14.0 ± 1.3 h
Nucleosome	6.0 ± 0.5	26 ± 4	57.8 ± 5.1 h	1.57 ± 0.13 h
-Fold change	1.1	2.1	4.7	0.11 (1/8.9)

[a] Photoproduct yields for free DNA are from two independent experiments (each shown), and for nucleosome DNA, yields are the average of three independent experiments with the standard deviations shown.

[b] Deamination half-lives were the average of those calculated from linear least squares fits to two (free DNA) or three (nucleosome DNA) independent sets of deamination data (7–9 time points each), with the error shown derived from propagation of the standard deviations for each fit (see supplemental Figs. S5 and S6).

the nucleosome did not affect the efficiency of forming the inside CPD, it enhanced the formation of the outside CPD by a factor of two.

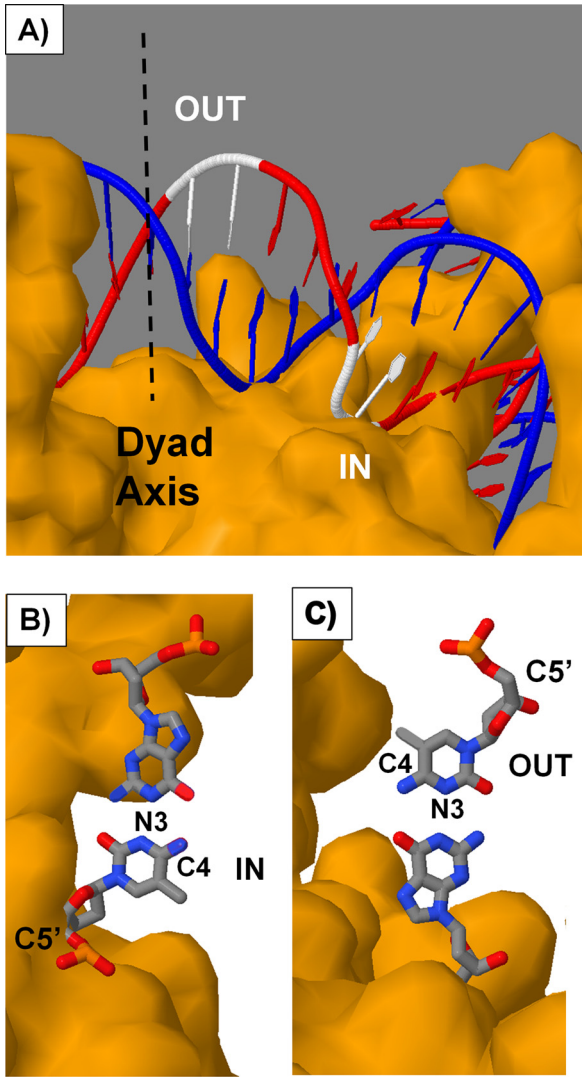

FIGURE 5. **Positions of the T^{m}CG sites on the nucleosome.** *A*, nucleosome core particle structure highlighting in *white* the positions of the inside and outside T^{m}CG CPD sites that are consistent with the hydroxyl radical footprinting data. *B* and *C*, orientation of the ^{m}C·G base pair for the inside (*B*) and outside (*C*) CPD sites. The structure was rendered from 1KX5.pdb (50) with Jmol using T1C2 and C6T7 of chain J to represent the outside and inside CPD sites with editing to produce the ^{m}CG base pair. The pseudo dyad axis is shown as a *dashed line*. It is also possible that the sites are displaced translationally by 10 bp to the other side of the dyad axis, but if so, they would only be present in minor amounts.

DISCUSSION

The aim of this study was to determine whether or not the rotational position of a *cis-syn*-cyclobutane dimer of a T^{m}CG site on a nucleosome would affect its deamination rate and thereby contribute to its relative mutagenicity via a deamination bypass mechanism. Two positions were studied, one with the phosphodiester backbone of the CPD against the histone core surface (IN) and one with the backbone away from the surface (OUT). These positions can be mapped onto a crystal structure of the nucleosome core particle as shown in Fig. 5*A*. Because the outside CPD site precedes the inside CPD site when going in the 5′- to 3′-direction, the two sites must lie to one side of the nucleosome pseudo dyad axis.

The photoreactivity of the two sites in free DNA (Table 1) was consistent with an earlier study of ours showing that an

AT^{m}CG site is about 2-fold more photoreactive than a GT-^{m}CG site (5.4 *versus* 12% yield) due to the quenching effect of flanking Gs (24). Complexing the DNA to the histone core particle did not affect the photoreactivity of the inside GT-^{m}CG site but enhanced the photoreactivity of the outside AT-^{m}CG site 2-fold to give a 26% yield of the CPD when compared with 5.5% for the inside site. The enhanced photoreactivity of the outside position is in accord with the higher photoreactivity previously noted for dipyrimidine sites positioned away from the histone surface (32, 33).

In contrast to their photoreactivity, the deamination rates of the two CPD sites in the nucleosome were dramatically different from those in the free DNA, with the CPD positioned inside deaminating 4.7 times slower and the CPD positioned outside deaminating 8.9 times faster (Table 1). The relative reactivity of the two CPDs toward deamination parallels the relative reactivity of the two CPD sites to hydroxyl radical cleavage, but we believe for a different reason. Although hydroxyl radical cleavage of DNA results mainly from initial abstraction of the hydrogens on the sugar backbone of DNA (49), deamination of an ^{m}C in a *cis-syn*-dimer involves attack of water on the C4 carbon (20), which lies in the major groove of the DNA.

Hydroxyl radical cleavage mainly involves attack at the C5′ position and 2–5-fold less at the other sugar sites in the order C4′ > C3′ > C2′ > C1′ (49). Maximum inhibition occurs when these hydrogens face toward the histone core surface, which sterically blocks the approach of the hydroxyl radical. Conversely, maximum cleavage is observed when the sugar hydrogens face out toward the solvent. When hydroxyl radical cleavage at a CPD is minimal (inside position), the sugar phosphate backbone faces the histone surface, but the C4 carbon of the ^{m}C faces in a direction parallel with the surface (Fig. 5*B*). On the other hand, when hydroxyl radical cleavage at the CPD is maximal (outside position), the sugar phosphate backbone faces away from the histone surface, but the C4 position of the ^{m}C faces in a direction parallel with the surface but in an opposite direction when compared with the CPD in the inside position (Fig. 5*C*).

Analysis of the crystal structure of a nucleosome core particle shows that the C4 position of what would be the ^{m}C of both the IN and the OUT CPDs is unobstructed by protein within a radius of 8.5 Å (1KX5.pdb) (50). The same would be expected to hold true for the CPDs as the 3′-pyrimidine of a CPD has been found to adopt roughly the same position as it does in the undamaged DNA (38). Thus, the C4 position of the ^{m}C of both the inside and the outside CPDs would appear to be in a similar, unobstructed environment, suggesting that factors other than steric interference by the histone proteins must play a role in inhibiting or enhancing deamination of the CPDs.

Previous studies of the deamination of C have found that deamination can be both inhibited and enhanced by protein binding. In one case, the α/β-type small, acid-soluble proteins of *Bacillus subtilis* spores have been found to suppress deamination by as much as 10-fold (51). It was suggested that the protein might be inhibiting deamination by a variety of means, such as restricting the "breathing" of the DNA, excluding water from the DNA, or enforcing an A conformation on the DNA. In a subsequent study, a restriction enzyme was found to both suppress and enhance deamination of Cs within its binding site by 7- and 15-fold, respectively (52). The large enhancement was proposed to arise from enzyme-mediated flipping of one of the Cs out of the helix. In addition, we recently showed that the methyl CpG binding domain of MeCP2 drastically inhibited deamination of a T^{m}CG CPD, most probably by restricting attack of water on the CPD (53).

In the case of the nucleosome, it may be that the same factors that increase CPD formation at outside positions also increase the deamination rate. It has been shown that CPD dimers form preferentially in outside positions in protein-free DNA loops, demonstrating that DNA curvature rather than protein-DNA contacts is controlling reactivity (34). It was suggested that the inside positions of curved DNA are more compressed and less mobile, whereas the outside positions are less compressed and more mobile. Thus, although the C4 positions of the ^{m}C in the inside and outside CPDs may be in similar steric environments, the increased flexibility and/or more open conformation of the outside position may facilitate protonation of N3 and/or attack by water at C4. Conversely, protonation of N3 or attack of water on C4 might be inhibited by restricted movements and the compressed nature of an inside CPD site. It is interesting to note that the observed rate of deamination of the outside CPD is very similar to if not faster than what we observed for a CPD with the same flanking bases in single strand DNA ($t_{1/2}$ = 1.57 *versus* 3.5 h). This could indicate that CPD might be able to flip out of the helix or is being held in a favorable conformation for deamination. A more detailed study of CPDs in different rotational and translational positions will be required to sort out these effects.

The 8.9-fold increase in the rate of deamination of an outside T^{m}CG dimer when compared with a 4.7-fold decrease for the inside dimer corresponds to an overall 42-fold difference in rate. When one couples the difference in deamination rate with a 2-fold enhancement of outside CPD formation, there would appear to be an 84-fold higher propensity for a UVB-induced ^{m}C to T mutation at an outside T^{m}CG site when compared with an inside site. Given that little difference has been observed in excision repair rates between inside and outside TT CPDs (41), the large difference in deamination rates could explain, at least in part, the origin of UV mutation hotspots and coldspots in phased nucleosomes that would arise following polymerase η bypass. On the other hand, deamination of an ^{m}C-containing CPD will result in a T·G mismatch, which has been shown to destabilize the DNA duplex by 0.7 kcal/mol (54). This duplex destabilization may further destabilize the nucleosome, which has already been shown to be destabilized by 0.14–0.24 kcal/mol by a TT CPD (41), and facilitate recognition by histone modification and/or excision repair systems. The extent of nucleosome destabilization, and hence recognition, may depend, however, on the rotational position of the mismatch. Deaminated C-containing CPDs have been shown to be much more readily detected and repaired than TT CPDs (55, 56).

CONCLUSION

We have found that the rotational position of a T^{m}CG CPD in a nucleosome greatly affects its deamination rate, and this may explain at least in part the origin of UV mutation hotspots and coldspots in phased nucleosomes. Deamination of CPDs may also be accelerated in unphased nucleosomes if the CPDs are in dynamic exchange with outside positions. It remains to been seen how the nucleosome affects the deamination rate of C^{m}CG CPDs, which are much more slowly deaminated than T^{m}CG CPDs in free DNA (24), as well as the deamination of (6-4) and Dewar photoproducts, which also form at this site (22). Rotational position is also expected to affect the spontaneous deamination of C and ^{m}C and their more readily deaminated oxidized products (57), as well as the chemistry of many other bases and adducts.

Acknowledgments—We thank Aziz Sancar for a gift of photolyase, Stephen Lloyd for a gift of T4 endonuclease V, and Michael Smerdon for a detailed protocol for preparation of the nucleosome core particles. We also thank John Hinz and Zeljko Svedruzic for helpful discussions on the design of the substrates.

REFERENCES

1. Brash, D. E., Rudolph, J. A., Simon, J. A., Lin, A., McKenna, G. J., Baden, H. P., Halperin, A. J., and Pontén, J. (1991) *Proc. Natl. Acad. Sci. U.S.A.* **88,** 10124–10128
2. Ziegler, A., Leffell, D. J., Kunala, S., Sharma, H. W., Gailani, M., Simon, J. A., Halperin, A. J., Baden, H. P., Shapiro, P. E., Bale, A. E., and Brash, D. E. (1993) *Proc. Natl. Acad. Sci. U.S.A.* **90,** 4216–4220
3. Giglia-Mari, G., and Sarasin, A. (2003) *Hum. Mutat.* **21,** 217–228
4. Pfeifer, G. P., You, Y. H., and Besaratinia, A. (2005) *Mutat. Res.* **571,** 19–31
5. Yoon, J. H., Lee, C. S., O'Connor, T. R., Yasui, A., and Pfeifer, G. P. (2000) *J. Mol. Biol.* **299,** 681–693
6. You, Y. H., and Pfeifer, G. P. (2001) *J. Mol. Biol.* **305,** 389–399
7. Cadet, J., Sage, E., and Douki, T. (2005) *Mutat. Res.* **571,** 3–17
8. Douki, T., and Cadet, J. (2001) *Biochemistry* **40,** 2495–2501
9. Tommasi, S., Denissenko, M. F., and Pfeifer, G. P. (1997) *Cancer Res.* **57,** 4727–4730
10. Drouin, R., and Therrien, J. P. (1997) *Photochem. Photobiol.* **66,** 719–726
11. You, Y. H., Li, C., and Pfeifer, G. P. (1999) *J. Mol. Biol.* **293,** 493–503
12. You, Y. H., Szabó, P. E., and Pfeifer, G. P. (2000) *Carcinogenesis* **21,** 2113–2117
13. You, Y. H., Lee, D. H., Yoon, J. H., Nakajima, S., Yasui, A., and Pfeifer, G. P. (2001) *J. Biol. Chem.* **276,** 44688–44694
14. Washington, M. T., Johnson, R. E., Prakash, S., and Prakash, L. (2000) *Proc. Natl. Acad. Sci. U.S.A.* **97,** 3094–3099
15. Yu, S. L., Johnson, R. E., Prakash, S., and Prakash, L. (2001) *Mol. Cell. Biol.* **21,** 185–188
16. McCulloch, S. D., Kokoska, R. J., Masutani, C., Iwai, S., Hanaoka, F., and Kunkel, T. A. (2004) *Nature* **428,** 97–100
17. Vu, B., Cannistraro, V. J., Sun, L., and Taylor, J. S. (2006) *Biochemistry* **45,** 9327–9335
18. Setlow, R. B. (1966) *Science* **153,** 379–386
19. Fix, D., and Bockrath, R. (1981) *Mol. Gen. Genet.* **182,** 7–11
20. Lemaire, D. G., and Ruzsicska, B. P. (1993) *Biochemistry* **32,** 2525–2533
21. Tu, Y., Dammann, R., and Pfeifer, G. P. (1998) *J. Mol. Biol.* **284,** 297–311
22. Douki, T., and Cadet, J. (1994) *Biochemistry* **33,** 11942–11950
23. Celewicz, L., Mayer, M., and Shetlar, M. D. (2005) *Photochem. Photobiol.* **81,** 404–418
24. Cannistraro, V. J., and Taylor, J. S. (2009) *J. Mol. Biol.* **392,** 1145–1157
25. Frederico, L. A., Kunkel, T. A., and Shaw, B. R. (1990) *Biochemistry* **29,** 2532–2537
26. Shen, J. C., Rideout, W. M., 3rd, and Jones, P. A. (1994) *Nucleic. Acids. Res.* **22,** 972–976
27. Taylor, J. S., and O'Day, C. L. (1990) *Biochemistry* **29,** 1624–1632
28. Jiang, N., and Taylor, J. S. (1993) *Biochemistry* **32,** 472–481
29. Lee, D. H., and Pfeifer, G. P. (2003) *J. Biol. Chem.* **278,** 10314–10321
30. Luger, K. (2006) *Chromosome Res.* **14,** 5–16
31. Luger, K., Mäder, A. W., Richmond, R. K., Sargent, D. F., and Richmond, T. J. (1997) *Nature* **389,** 251–260
32. Gale, J. M., Nissen, K. A., and Smerdon, M. J. (1987) *Proc. Natl. Acad. Sci. U.S.A.* **84,** 6644–6648
33. Pehrson, J. R. (1989) *Proc. Natl. Acad. Sci. U.S.A.* **86,** 9149–9153
34. Pehrson, J. R., and Cohen, L. H. (1992) *Nucleic. Acids Res.* **20,** 1321–1324
35. Becker, M. M., and Wang, Z. (1989) *J. Mol. Biol.* **210,** 429–438
36. Pfeifer, G. P. (1997) *Photochem. Photobiol.* **65,** 270–283
37. Suquet, C., and Smerdon, M. J. (1993) *J. Biol. Chem.* **268,** 23755–23757
38. Park, H., Zhang, K., Ren, Y., Nadji, S., Sinha, N., Taylor, J. S., and Kang, C. (2002) *Proc. Natl. Acad. Sci. U.S.A.* **99,** 15965–15970
39. Kosmoski, J. V., and Smerdon, M. J. (1999) *Biochemistry* **38,** 9485–9494
40. Kosmoski, J. V., Ackerman, E. J., and Smerdon, M. J. (2001) *Proc. Natl. Acad. Sci. U.S.A.* **98,** 10113–10118
41. Svedružić, Z. M., Wang, C., Kosmoski, J. V., and Smerdon, M. J. (2005) *J. Biol. Chem.* **280,** 40051–40057; Correction (2010) *J. Biol. Chem.* **285,** 39574
42. Thoma, F. (2005) *DNA Repair* **4,** 855–869
43. Wang, Z. G., Wu, X. H., and Friedberg, E. C. (1991) *J. Biol. Chem.* **266,** 22472–22478
44. Hara, R., and Sancar, A. (2003) *Mol. Cell. Biol.* **23,** 4121–4125
45. Liu, X., and Smerdon, M. J. (2000) *J. Biol. Chem.* **275,** 23729–23735
46. Ober, M., and Lippard, S. J. (2007) *J. Am. Chem. Soc.* **129,** 6278–6286
47. Li, Q., and Wrange, O. (1993) *Genes Dev.* **7,** 2471–2482
48. Li, Q., and Wrange, O. (1995) *Mol. Cell. Biol.* **15,** 4375–4384
49. Balasubramanian, B., Pogozelski, W. K., and Tullius, T. D. (1998) *Proc. Natl. Acad. Sci. U.S.A.* **95,** 9738–9743
50. Davey, C. A., Sargent, D. F., Luger, K., Maeder, A. W., and Richmond, T. J. (2002) *J. Mol. Biol.* **319,** 1097–1113
51. Sohail, A., Hayes, C. S., Divvela, P., Setlow, P., and Bhagwat, A. S. (2002) *Biochemistry* **41,** 11325–11330
52. Carpenter, M., Divvela, P., Pingoud, V., Bujnicki, J., and Bhagwat, A. S. (2006) *Nucleic Acids Res.* **34,** 3762–3770
53. Cannistraro, V. J., and Taylor, J. S. (2010) *Nucleic. Acids. Res.* **38,** 6943–6955
54. Jing, Y., Kao, J. F., and Taylor, J. S. (1998) *Nucleic. Acids. Res.* **26,** 3845–3853
55. Mu, D., Tursun, M., Duckett, D. R., Drummond, J. T., Modrich, P., and Sancar, A. (1997) *Mol. Cell. Biol.* **17,** 760–769
56. Sugasawa, K., Okamoto, T., Shimizu, Y., Masutani, C., Iwai, S., and Hanaoka, F. (2001) *Genes Dev.* **15,** 507–521
57. Kreutzer, D. A., and Essigmann, J. M. (1998) *Proc. Natl. Acad. Sci. U.S.A.* **95,** 3578–3582